On the fracture behaviour of aerospace-grade Polyether-ether-ketone composite-to-aluminium adhesive joints

Quan, Dong; Wang, Guilong; Zhao, Guoqun; Alderliesten, René

DOI
10.1016/j.coco.2022.101098

Publication date
2022

Document Version
Final published version

Published in
Composites Communications

Citation (APA)
Quan, D., Wang, G., Zhao, G., & Alderliesten, R. (2022). On the fracture behaviour of aerospace-grade Polyether-ether-ketone composite-to-aluminium adhesive joints. *Composites Communications*, *30*, Article 101098. https://doi.org/10.1016/j.coco.2022.101098

Composites Communications 30 (2022) 101098

Contents lists available at ScienceDirect

Composites Communications

journal homepage: www.elsevier.com/locate/coco

Short communication

On the fracture behaviour of aerospace-grade Polyether-ether-ketone composite-to-aluminium adhesive joints

Dong Quan [a,*], Guilong Wang [a], Guoqun Zhao [a], René Alderliesten [b]

[a] *Key Laboratory for Liquid-Solid Structural Evolution and Processing of Materials (Ministry of Education), Shandong University, China*
[b] *Structural Integrity & Composites Group, Delft University of Technology, Netherlands*

ARTICLE INFO

Keywords:
Aerospace composite-to-metal joints
Adhesive joining
Surface treatment
Fracture behaviour

ABSTRACT

The inherently low surface energy of carbon fibre reinforced Polyether-ether-ketone (CF/PEEK) composites results in an extremely low compatibility with adhesives. This subsequently causes significant challenges in the adhesive joining of them to other dissimilar materials. Herein, the bonding surfaces of the CF/PEEK composites were treated by a high-power UV-irradiation technique prior to the adhesive bonding, with an attempt to develop hybrid composite-to-aluminium joints with excellent fracture resistance. The mode-I, mode-II and mix-mode fracture behaviour of CF/PEEK-to-aluminium joints bonded by two commercial aerospace adhesives was evaluated. Cohesive failure within the adhesive layers or substrate damage to the CF/PEEK composites were observed in all the cases. This indicated that the adhesion between the CF/PEEK composites and the adhesives was sufficient to prevent an adhesive failure at the composite/adhesive interfaces under different fracture modes. This study explored an effective route to develop strong and tough CF/PEEK-to-aluminium joints for aerospace applications. Additionally, it revealed that the form of the adhesive supporting carrier was a key factor affecting the fracture behaviour and fracture energies of the adhesive joints.

1. Introduction

The usage of carbon fibre reinforced thermoplastic composites (TPCs) in aerospace industry has extensively expanded over the last decade, with a more rapid growth being foreseen in a short future. Consequently, a combined usage of components based on TPCs, thermoset composites (TSCs) and metal alloys (such as titanium and aluminium) becomes a major development trend for modern aircrafts. The different characteristics of TPCs, TSCs and metal alloys bring in a challenge of developing effective joining methods for cost-effective assembly. Mechanical fastening [1,2] and adhesive bonding [3,4] are currently the two main methods for joining aerospace components, while infusion bonding [5,6] is still under development and validation for major aerospace applications. Adhesive bonding offers many advantages over the other joining methods, including a possibility for avoiding high stress concentration at the bonding junction, obtaining a continuous bonding that seals the entire bonding area, adding negligible weight to the joints and effectively joining large scale thin-walled components [7,8]. Accordingly, it is considered as the most suitable joining methods for composite materials, especially for the bonding of composite-to-metal joints.

As a high performance non-crystalline thermoplastics, Polyether ether ketone (PEEK) possessed exceptional mechanical properties, excellent fracture toughness, outstanding thermal and chemical stabilities. For these reasons, carbon fibre reinforced PEEK (CF/PEEK) composites are among the most widely used TPCs for advanced aerospace applications. However, the intrinsically low surface polarities of the PEEK plastics resulted in an extremely low adhesion/miscibility with structural adhesives, i.e. the failure strength of the adhesively bonded CF/PEEK composites without surface treatment was very poor [9]. Accordingly, the development of effective surface treatment methods to promote the surface activities of the CF/PEEK composites becomes crucial. In previous studies [9,10], a high-power UV-irradiation technique was proposed to rapidly prepare the surfaces of the CF/PEEK composites for adhesive bonding. It had proved to significantly enhance the adhesion between the composites substrates and the structural adhesives by applying a UV-treatment to the CF/PEEK composites for a short period. For example, hybrid CF/PEEK-to-aluminium (Al) joints with remarkably increased lap-shear strengths were obtained by rapidly UV-irradiating the surfaces of the PEEK composites for 5–20 s [10] prior to the joining process. Moreover, an analysis on the failure surfaces of the lap-shear adhesive joints revealed that the failure mode transferred from adhesive failure at the TPC/adhesive interface to

---

* Corresponding author.
E-mail address: quandong@sdu.edu.cn (D. Quan).

https://doi.org/10.1016/j.coco.2022.101098
Received 28 November 2021; Received in revised form 29 January 2022; Accepted 7 February 2022

substrate damage of the CF/PEEK composites upon the UV-irradiation [10]. The results of the previous work [10] highlighted high-power UV-irradiation a very promising method for surface preparation of CF/PEEK composites for their adhesive joining with Al alloys. However, only the lap-shear strengths of the adhesive joints were studied in [10], while the failure of the practical adhesive joints usually took place in fracture modes, especially for the large-scale thin-wall joints with big bonding areas [7,11]. More critically, the presence of a crack in an adhesive joint causes a high stress concentration in the vicinity of the crack tip, that often leads to crack growth and ultimately failure at an applied stress below the failure strength of the adhesives [7,11]. Accordingly, to further develop this joining technique towards industrial mass-production, it is critical to investigate the fracture behaviour and mechanisms of the hybrid TPC-to-Al adhesive joints. Noteworthily, based on a comprehensive literature review, there is still a serious lack of studies on the fracture behaviour of hybrid TPC-to-metal joints. Herein, hybrid joints between CF/PEEK composites and aluminium 2024-T3 alloys bonded by two aerospace film adhesives were prepared, with the CF/PEEK composites being UV-irradiated prior to the adhesive joining. The mode-I, mode-II and mix-mode fracture behaviour of the CF/PEEK-to-Al joints were investigated, and the fracture mechanisms were also studied to investigate whether sufficient adhesion was obtained at the composite/adhesive interface to prevent any interface failure. The experimental results had demonstrated that hybrid CF/PEEK-to-Al joints with excellent fracture resistance can be produced by the proposed joining method.

2. Experimental

2.1. Materials and sample preparation

The Al substrates were alloy 2024-T3 supplied by Fokker Technologies of GKN Aerospace Services Limited, the Netherlands. The surfaces of the aluminium substrates were treated by a Stuart–Bengough chromic acid anodising process, that ensured a good adhesion between the structural adhesives and the aluminium substrates. PEEK powder-coated 5-harness satin weave prepregs supplied by TenCate Advanced Composites were used to produce the CF/PEEK composites. A $[0°/90°]_{6S}$ layup with an in-plane dimension of 600 mm × 600 mm was consolidated in a Joos LAP100 hot-platen press at 2 MPa and 390 °C for 30 min, see Fig. 1 (a).

Prior to the bonding, a UV-treatment lasting for different durations was applied to the bonding surfaces of the CF/PEEK substrates within an enclosed chamber that was equipped a LH6 MKII UV source (200 W/cm) and a Mercury D bulb, as shown in Fig. 1 (b). The intensities of the UV lights applied to the CF/PEEK surfaces were measured to be 2132 mW/cm^2, 1678 mW/cm^2, 349 mW/cm^2 and 57 mW/cm^2 for the UVV (395–445 nm), UVA (320–390 nm), UVB (280–320 nm) and UVC (250–260 nm), respectively using a UV Power Puck from EIT Inc., USA. A series of trials have been carried out by varying the durations of the UV treatment, with the surface free energies and water contact angles of the CF/PEEK being measured using a mobile surface analyser from KRÜSS, GmbH. These trials aimed to identify a minimum treatment time that was sufficient to ensure a good adhesion between the adhesives and the CF/PEEK composites. It was observed that applying a 7 s UV treatment to the CF/PEEK surface decreased its water contact angle from 82.19° to 65.48°, and increased the polar component of the surface energy from 3.69 mN/m to 6.26 mN/m. These levels of surface wettability and polarity satisfied the requirements based on the results of our previous work [9,10].

After the 7 s UV-treatment, two epoxy film adhesives, i.e. Scotch-Weld^{TM} AF163-2K and AF163-2OST from 3M were used to bond the CF/PEEK substrates and the Al substrates. Both of the two film adhesives belonged to the family of Scotch-Weld^{TM} AF163-2 that were commercialised for aerospace structural applications. They possessed the same adhesive matrix but different supporting carriers, i.e. the supporting carrier was non-woven thermoplastic fibres for the AF163-2OST, and thermoplastic fibre knit for the AF163-2K. During the sample preparation, one layer of film adhesive was inserted between one piece of CF/PEEK substrate and one piece of Al substrate to prepare a joint assembly for the following curing process, see Fig. 1 (c). A piece of PTFE film with a thickness of 12.5 μm was also placed above the adhesive layer to generate crack starters in the specimens for the following fracture tests. The adhesive joint assembly was then sealed in a vacuum bag and placed in an autoclave for curing, as shown in Fig. 1 (d). The curing cycle of the adhesive joints was a single dwell step at 121 °C and 0.3 MPa gauge pressure for 90 min, and a 0.073 MPa under pressure inside the vacuum bag was also used throughout the curing process. After the curing, the adhesive joints were machined into desired dimensions for the fracture tests. Noteworthily, reference adhesive joints with non-treated CF/PEEK substrates were also prepared using the same procedure. However, all the reference joints failed during the machining process, owing to the very poor adhesion between the non-treated CF/PEEK substrates and the adhesives. The thickness of the Al 2024-T3 alloy and the CF/PEEK composite was 1.6 mm and 2.0 mm, respectively. This configuration of the adhesive joints was designed by following the criterion of matching the flexural stiffnesses of the two adherends, so as to ensure essentially accurate mode-mixity in the following fracture tests. It is worthy to mention that the deviation in the longitudinal strain of the two adherends (due to their different elastic modulus) [12,13] and the presence of residual thermal stresses in the adhesive joints (caused by the different coefficients of thermal expansion of the two adherends) [14–16] can also lead to an off-set in the mode-mixity of the fracture tests. However, these affecting factors were ignored in the current work.

2.2. Fracture tests and failure analysis

The mode-I, mode-II and mix-mode fracture properties of the adhesively bonded CF/PEEK-to-Al joints were studied using a double cantilever beam (DCB) test [17], an end loaded split (ELS) test [18] and a fixed-ratio mixed-mode (FRMM) test [11], respectively. The mode-mixity of the FRMM test, i.e. mode-I/mode-II was 57%/43% [11]. The illustrations and specimen dimensions of these tests are shown in Figs. 1 (e)–(g). All the tests were carried out at a constant displacement rate of 4 mm/min, with the crack length being monitored using a high resolution digital camera during the testing. At least three replicable tests were performed for each set of adhesive joints. The fracture toughness, G_C, was calculated using a corrected beam theory (CBT) analysis from Eq. (1) for the DCB test, Eq. (2) for the ELS test and Eq. (3a)–(3c) for the FRMM test.

$$G_{IC} = \frac{3P\delta}{2b(a+|\Delta_I|)}\frac{F}{N} \tag{1}$$

$$G_{IIC} = \frac{9P^2(a+|\Delta_{II}|)^2}{4b^2h^3E_f}\cdot F \tag{2}$$

$$G_{I/IIC} = G_I + G_{II} \tag{3a}$$

$$G_I = \frac{3P^2(a+|\Delta_I|)^2}{b^2E_fh^3}\cdot F \tag{3b}$$

$$G_{II} = \frac{9P^2(a+|\Delta_{II}|)^2}{4b^2h^3E_f}\cdot F \tag{3c}$$

where P is the load, δ is the load point displacement, b is specimen width, a is the precrack length, h is the thickness of the beam and E_f is the flexural modulus. F, N and Δ_I/Δ_{II} are the correction factors for large displacements, load block effects and root rotation of the crack tip, respectively, as detailed in [17,18]. To investigate the failure mode and fracture mechanisms of the adhesive joints, a JSM-7500F scanning electron microscope (SEM) was used to image the fracture surfaces after the fracture tests.

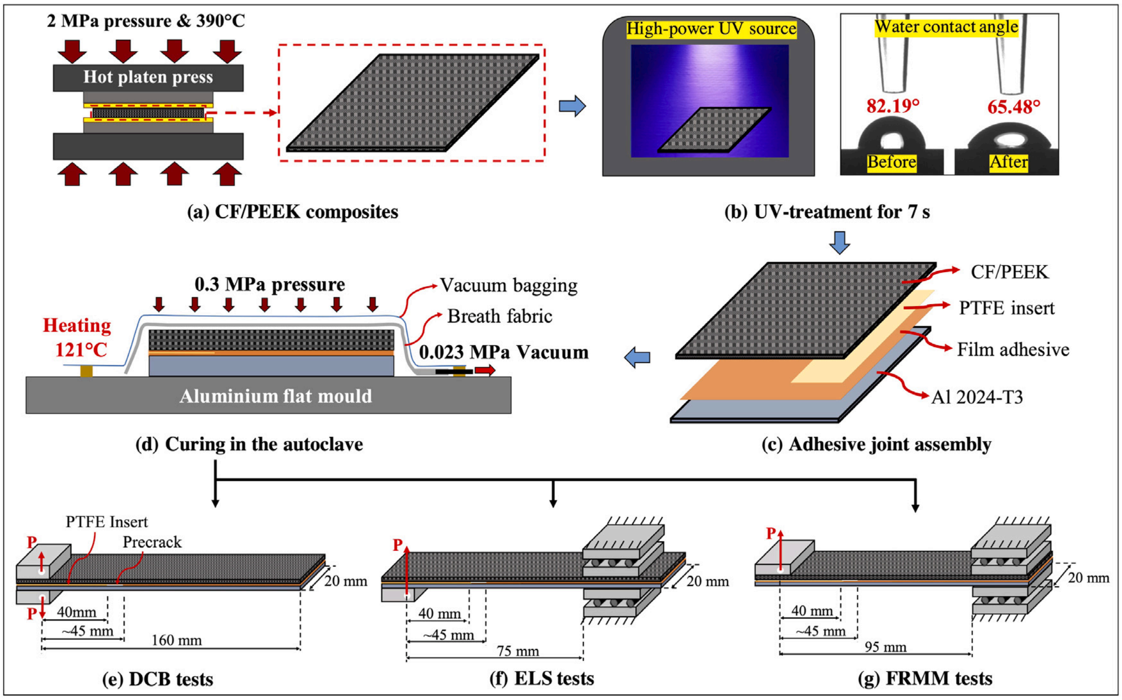

Fig. 1. Illustrations for the sample preparation and fracture tests of the adhesive joints.

3. Results and discussion

3.1. Failure mode of the adhesive joints

Fig. 2 shows photographs and microscopy images of the fracture surfaces of the AF163-2OST adhesive joints. The colour of the cured AF163-2OST adhesive was light green. From the photographs of the mode-I, mode-II and mix-mode fracture surfaces, it was observed that both sides of the fractured specimens were attached with a layer of green colour adhesive. Additionally, the representative SEM images showed that there were a large number of broken and debonded fibres on the fracture surfaces of the AF163-2OST adhesive joints in all the cases. These fibres were the thermoplastic fibres that made up of the non-woven supporting carriers of the AF163-2OST adhesives. Based on these observations, it was obvious that the crack propagated cohesively inside the adhesive layers during the fracture processes of the AF163-2OST adhesive joints in all the cases. Moreover, extensive debonding, bridging and breakage of the supporting thermoplastic fibres took place during the cohesive failure of the adhesive joints, as illustrated by the inset image at the bottom of Fig. 2. The joints bonded by the AF163-2K adhesives exhibited significantly different types of failure mode as the AF163-2OST adhesive joints. Representative photographs and microscopy images of the fracture surfaces of the AF163-2K adhesive joints are shown in Fig. 3. The colour of the AF163-2K adhesive was red. As can been seen from the photographs of the fracture surfaces, the entire red colour adhesive layers were left on the Al sides of the fracture surfaces in all the cases. Additionally, the adhesive layers were all decorated with a large amount of PEEK debris, that were peeled-off from the CF/PEEK substrates. By taking a closer look at the SEM images in Fig. 3, evidence of carbon fibre breakage was observed on the fracture surfaces of the composite sides. These phenomena indicated that a substrate damage to the CF/PEEK substrates occurred during the fracture process of the AF163-2K adhesive joints. This was associated with the peeling-off of the PEEK resin from the CF/PEEK composite substrates and carbon fibre breakage during the fracture process, as schematically shown by the inset image at the bottom of Fig. 3.

The above observations clearly demonstrated that excellent adhesion at the interface between the adhesives and the CF/PEEK composites was obtained upon applying a rapid UV treatment (lasting for only 7 s) to the composite substrates. More importantly, the level of the adhesion was sufficient to prevent a failure at the adhesive/composite interfaces in all the cases. However, the question that arise was why the AF163-2OST adhesive joints and the AF163-2K adhesive joints exhibited significantly different failure modes . As mentioned in Section 2.1, the only difference between the two adhesives was the supporting carrier, i.e. thermoplastic non-woven for the AF163-2OST adhesive, and thermoplastic fibre knit for the AF163-2K adhesive. During the fracture processes, the crack always propagated along the weakest path at the mid-plane. For the AF163-2K adhesive, the thermoplastic fibres of the knit carrier were in a continuous and well-structured form, that formed a strong structure within the adhesive layer and prevented a cohesive failure (see the inset image at the bottom of Fig. 3). Accordingly, the crack was migrated into the CF/PEEK substrates. In contrast, the supporting carrier of the AF163-2OST adhesive was consisted of randomly distributed thermoplastic discontinuous fibres (see the inset image at the bottom of Fig. 2.), and hence it possessed relatively low failure strength. In this case, the crack was easily diverted into the adhesive layers, and remained within it while propagating forward.

3.2. Fracture energies of the adhesive joints

The load versus displacement curves of all the fracture tests are shown in Figs. 4 (a)–(c). In general, a steady crack propagation failure mode was observed during the mode-I, mode-II and mix-mode fracture processes of the AF163-2OST adhesive joints. This corresponded to the relatively smooth load versus displacement curves in Figs. 4 (a)–(c). In contrast, typical non-steady crack propagation behaviour was observed for the AF163-2K joints in all the cases. In specific, a stick–slip fracture behaviour was observed for the DCB tests, resulting in 'saw-teeth' shape load versus displacement curves (Fig. 4 (a)). The ELS specimens failed dynamically (the crack suddenly jumped to the end of the specimens) after the crack propagated for about 3 mm, resulting

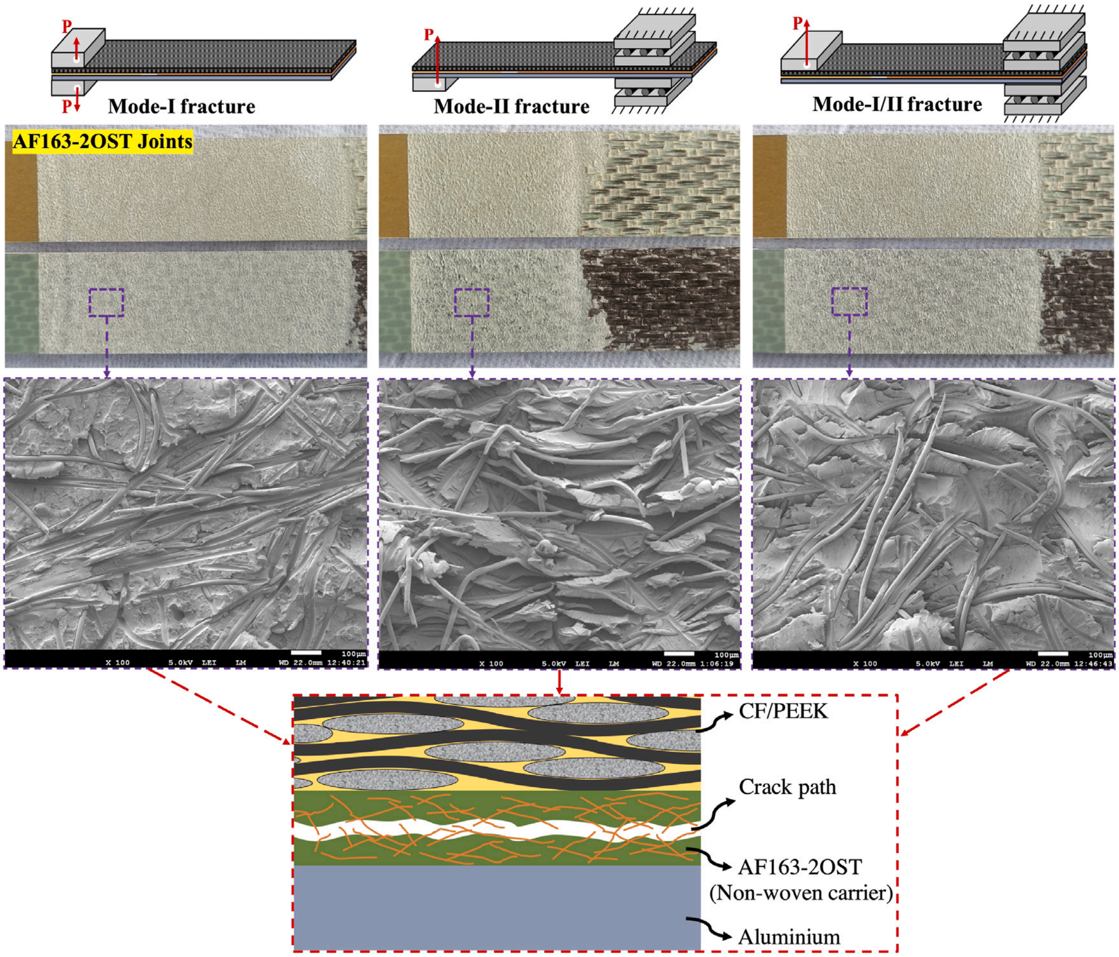

Fig. 2. Representative photographs and microscopy images of the fracture surfaces of the AF163-2OST joints. (For interpretation of the references to colour in this figure legend, the reader is referred to the web version of this article.)

in a sharp drop of the load versus displacement curves at the peak (Fig. 4(b)). Similarly, a sudden drop in the load versus displacement curves was also observed for the FRMM specimens of the AF163-2K joints, corresponding to a dynamic failure during the tests (Fig. 4(c)). The different mechanical responses of the fracture specimens between the AF163-2OST joints and the AF163-2K joints were attributed to the different architectures of the crack paths. For the AF163-2OST joints, the crack propagated within the adhesive layers, in which, the debonding, pulling-out and bridging mechanisms of the numerous thermoplastic fibres (as observed in Fig. 2) prevented obvious jumping of the crack. However, the dominating failure phenomenon of the AF163-2K joints was the peeling-off of PEEK resins from the carbon fibre woven of the CF/PEEK substrates, as shown in Fig. 3. In this case, the lack of resins and local non-uniformity caused by the woven-style of the carbon fibres lead to non-stable crack propagation of the adhesive joints. Additionally, a dynamic failure of the mode-II and mix-mode fracture specimens was typically associated with significant extension in the length of the fracture process zone ahead of the crack tip [19,20]. In this case, an extended fracture process zone normally happened to the materials with good mechanical properties under shearing, that typically resulted in relatively high fracture energies of the mode-II and mix mode-I/mode-II fracture energies [19,20].

Table 1
Fracture energy value of each specimen (indicated by S1–S3) and the corresponding average values from the DCB, ELS and FRMM tests of the adhesive joints.

Items		G_{IC} (J/m^2)	G_{IIC} (J/m^2)	$G_{I/IIC}$ (J/m^2)
AF163-2OST	S1	1235	3522	1670
	S2	1120	3352	1744
	S3	1156	3406	1763
	Mean	1170 ± 59	3427 ± 87	1736 ± 32
AF163-2K	S1	667	5794	3179
	S2	796	6626	2872
	S3	680	6862	3065
	Mean	715 ± 71	6428 ± 561	3039 ± 155

Figs. 4(d)–(f) present the corresponding R-curves obtained from the fracture tests. Noteworthily, only a limited number of values were recorded during the mode-I, mode-II and mix-mode fracture tests of the AF163-2K joints, as a result of the non-stable crack propagations. Additionally, an obvious rising trend of the R-curves was observed for the mode-II fracture of the AF163-2K joints, indicating a significant extension in the length of the fracture process zone. The mode-I, mode-II and mix-mode fracture energies of the adhesive joints obtained from the R-curves are shown in Table 1. It should be noted that G_{IIC} of the AF163-2K joints were taken as the values prior to the dynamic failure, i.e. the maximum values on the corresponding R-curves. It was observed that the AF163-2OST joints possessed a much higher G_{IC} than the AF163-2K joints. This was because of the debonding, breakage and bridging mechanisms of the thermoplastic fibres were highly effective for energy dissipation during a mode-I opening fracture [21,22], and subsequently increased the fracture energies of the adhesive joints. However, a typical low surface energy of the thermoplastic fibres cased

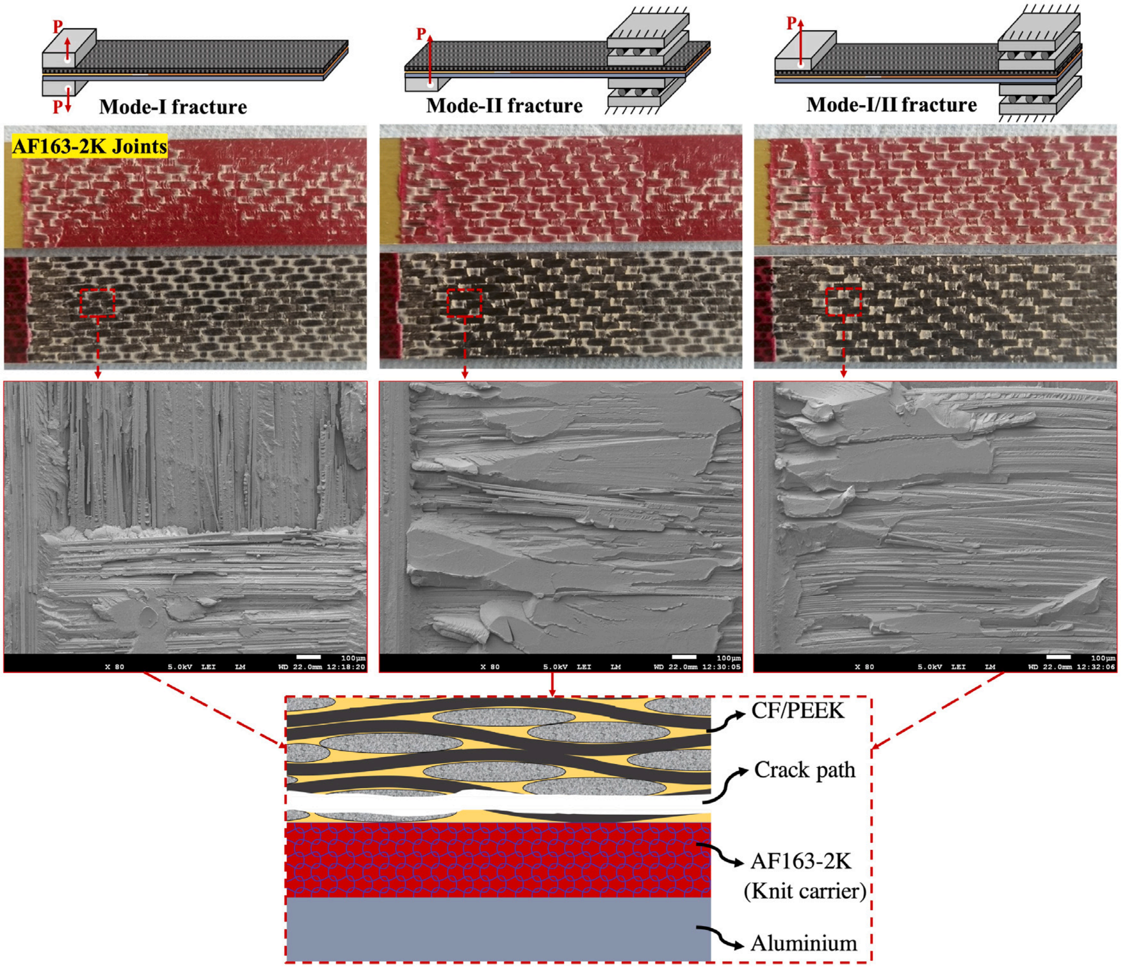

Fig. 3. Representative photographs and microscopy images of the fracture surfaces of the AF163-2K joints. (For interpretation of the references to colour in this figure legend, the reader is referred to the web version of this article.)

a relatively weak adhesion at the interface between the individual thermoplastic fibres and the epoxy adhesive matrix. This negatively affected the shearing properties of the AF163-2OST adhesive layers. This explained why the values of G_{IIC} and $G_{I/IIC}$ of the AF163-2K joints were 88% and 75% higher than that of the AF163-2OST joints. Overall, the different crack propagation modes of the adhesive joints (that was determined by the different types of supporting carriers of the adhesives) had significant effects on the fracture energies. It is worthy to mention that, based on the best knowledge of the authors, there is no other literature that investigated the fracture energies of hybrid adhesive joints between aerospace grade thermoplastic composites and metals to date. Accordingly, it was not possible to compare the measured fracture energy values with the results of any other work. However, the failure modes of the adhesive joints, i.e. either cohesive failure or substrate damage clearly demonstrated that excellent fracture performance of the adhesive joints had been obtained for the given CF/PEEK-to-Al material combinations.

4. Conclusions

This work aimed at developing hybrid adhesive joints between carbon fibre reinforced Polyether-ether-ketone (CF/PEEK) composite and aluminium 2024-T3 with high fracture resistance. Two commercial aerospace film adhesives, namely AF163-2OST and AF163-2K, were used for the bonding. The main difference between the adhesives was the form of the adhesive supporting carrier, i.e. the supporting carrier of the AF163-2OST adhesive was thermoplastic non-woven and the AF163-2K adhesive used a thermoplastic knit as the supporting carrier. An analysis on the failure mode of the adhesive joints had demonstrated that a rapid UV-treatment lasting for 7 s on the CF/PEEK substrates was sufficient to improve the adhesion of the adhesives with the CF/PEEK substrates. During the mode-I, mode-II and mix-mode fracture processes, it prevented the failure of the adhesive joints at the adhesive/composite interface, and migrated the crack into the adhesive layers for the AF163-2OST joints or the CF/PEEK substrates for the AF163-2K joints. This essentially meant that a highest structural integrity of the adhesive joints that can be achieved by using a surface treatment method had been obtained. The results of the fracture tests also highlighted the form of the supporting carrier a critical factor affecting the crack propagation behaviour and fracture energies of the adhesive joints. This observation should be carefully considered for the engineering applications of adhesives, e.g. proper supporting carriers shall be selected based on the type of load the adhesive joints is going to bear during their service life. Overall, advanced aerospace-grade adhesive joints between CF/PEEK composite and aluminium with excellent fracture performance had been developed by applying a rapid UV treatment to the CF/PEEK substrates.

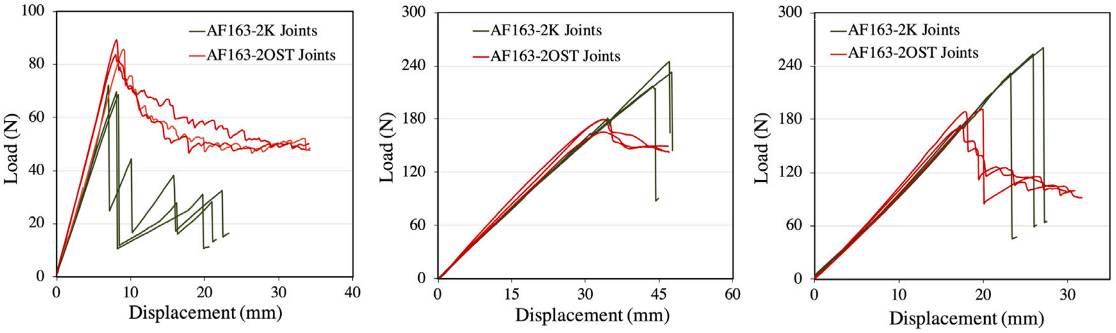

(a) DCB (b) ELS (c) FRMM

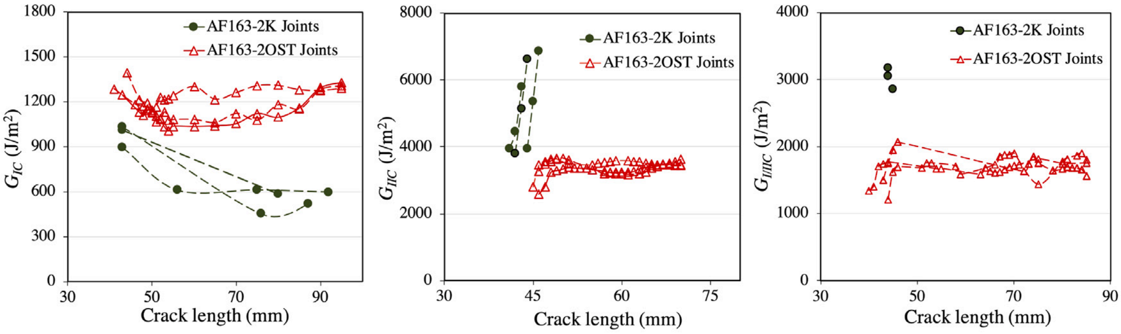

(d) DCB (e) ELS (f) FRMM

Fig. 4. The load versus displacement curves (a–c) and corresponding *R*-curves (d–f) of the DCB, ELS and FRMM tests. (For interpretation of the references to colour in this figure legend, the reader is referred to the web version of this article.)

CRediT authorship contribution statement

Dong Quan: Conceptualization, Investigation, Funding acquisition, Writing – original draft. **Guilong Wang:** Methodology, Funding acquisition. **Guoqun Zhao:** Conceptualization, Writing – review & editing. **René Alderliesten:** Project administration, Writing – review & editing.

Declaration of competing interest

The authors declare that they have no known competing financial interests or personal relationships that could have appeared to influence the work reported in this paper.

Acknowledgements

The authors would like to acknowledge the financial supports from the key research and development program of Shandong Province, China (Grant No. 2021ZLGX01). The authors thank to Dr. Brian Deegan from Adhesives Research, Henkel Ireland Operations & Research Ltd. for the many valuable comments and suggestions provided. Dr. Dong Quan is grateful to the European Union's Horizon 2020 research and innovation programme under the Marie Skłodowska-Curie grant agreement No. 842467. Guilong Wang is grateful to the National Natural Science Foundation of China (NSFC, Grant No. 51875318, 52175341) and Shandong Provincial Key Research and Development Program, China (Major Scientific and Technological Innovation Project) (Grant No. 2019JZZY020205).

References

[1] Ali Mehboob, Seung-Hwan Chang, Effect of composite bone plates on callus generation and healing of fractured tibia with different screw configurations, Compos. Sci. Technol. 167 (2018) 96–105, http://dx.doi.org/10.1016/j.compscitech.2018.07.039.

[2] Yanfeng Zhang, Zhengong Zhou, Shidong Pan, Zhiyong Tan, Comparison on failure behavior of three-dimensional woven carbon/carbon composites joints subjected to out-of-plane loading at room and high temperature, Compos. Commun. 23 (2021) 100567, http://dx.doi.org/10.1016/j.coco.2020.100567.

[3] Ting Zhang, Jia Meng, Qing Pan, Baozhong Sun, The influence of adhesive porosity on composite joints, Compos. Commun. 15 (2019) 87–91, http://dx.doi.org/10.1016/j.coco.2019.06.011.

[4] Thulasidhas Dhilipkumar, Murugan Rajesh, Enhancing strength and stiffness of composite joint through co-cure technique, Compos. Commun. 27 (2021) 100878, http://dx.doi.org/10.1016/j.coco.2021.100878.

[5] Goram Gohel, Somen K. Bhudolia, Jayaram Kantipudi, Kah Fai Leong, Robert J. Barsotti, Ultrasonic welding of novel carbon/elium with carbon/epoxy composites, Compos. Commun. 22 (2020) 100463, http://dx.doi.org/10.1016/j.coco.2020.100463.

[6] Hot gas implant welding of polypropylene via a three-dimensional porous copper implant, Compos. Commun. 25 (2021) 100761, http://dx.doi.org/10.1016/j.coco.2021.100761.

[7] A.J. Kinloch, Adhesion and Adhesives: Science and Technology, Chapman and Hall, 1987.

[8] A. Pramanik, A.K. Basak, Y. Dong, P.K. Sarker, M.S. Uddin, G. Littlefair, A.R. Dixit, S. Chattopadhyaya, Joining of carbon fibre reinforced polymer (CFRP) composites and aluminium alloys–A review, Compos. A 101 (2017) 1–29, http://dx.doi.org/10.1016/j.compositesa.2017.06.007.

[9] Dong Quan, Rene Alderliesten, Clemens Dransfeld, Ioannis Tsakoniatis, Sofia Teixeira De Freitas, Gennaro Scarselli, Neal Murphy, Alojz Ivankovic, Rinze Benedictus, Significantly enhanced structural integrity of adhesively bonded PPS and PEEK composite joints by rapidly UV-irradiating the substrates, Compos. Sci. Technol. 199 (2020) 108358, http://dx.doi.org/10.1016/j.compscitech.2020.108358.

[10] Dong Quan, Brian Deegan, Lorcan Byrne, Gennaro Scarselli, Alojz Ivankovic, Neal Murphy, Rapid surface activation of carbon fibre reinforced PEEK and PPS composites by high-power UV-irradiation for the adhesive joining of dissimilar materials, Compos. A 137 (2020) 105976, http://dx.doi.org/10.1016/j.compositesa.2020.105976.

[11] B.R.K. Blackman, A.J. Kinloch, Fracture tests for structural adhesive joints, in: D.R. Moore, A. Pavan, J.G. Williams (Eds.), Fracture Mechanics Testing Methods for Polymers, Adhesives and Composites, Elsevier Science, Amsterdam, 2001, pp. 225–270.

[12] Zhenyu Ouyang, Gefu Ji, Guoqiang Li, On approximately realizing and characterizing pure mode-I interface fracture between bonded dissimilar materials, J. Appl. Mech. 78 (3) (2011) 031020, http://dx.doi.org/10.1115/1.4003366.

[13] Wandong Wang, Romina Lopes Fernandes, Sofia Teixeira De Freitas, Dimitrios Zarouchas, Rinze Benedictus, How pure mode I can be obtained in bi-material bonded DCB joints: A longitudinal strain-based criterion, Compos. B 153 (2018) 137–148, http://dx.doi.org/10.1016/j.compositesb.2018.07.033.

[14] Tomohiro Yokozeki, Energy release rates of bi-material interface crack including residual thermal stresses: Application of crack tip element method, Eng. Fract. Mech. 77 (1) (2010) 84–93, http://dx.doi.org/10.1016/j.engfracmech.2009.09.018.

[15] Panayiotis Tsokanas, Theodoros Loutas, Hygrothermal effect on the strain energy release rates and mode mixity of asymmetric delaminations in generally layered beams, Eng. Fract. Mech. 214 (2019) 390–409, http://dx.doi.org/10.1016/j.engfracmech.2019.03.006.

[16] Panayiotis Tsokanas, Theodoros Loutas, Georgios Kotsinis, Vassilis Kostopoulos, Wouter M. van den Brink, Federico Martin de la Escalera, On the fracture toughness of metal-composite adhesive joints with bending-extension coupling and residual thermal stresses effect, Compos. B 185 (2020) 107694, http://dx.doi.org/10.1016/j.compositesb.2019.107694.

[17] BS 7991:2001, Determination of the Mode I Adhesive Fracture Energy, GIC, of Structural Adhesives Using the Double Cantilever Beam (DCB) and Tapered Double Cantilever Beam (TDCB) Specimens, British Standard Institute, 2001.

[18] ISO 15114:2014, Fibre-Reinforced Plastic Composites-Determination of Mode II Fracture Resistance for Unidirectionally Reinforced Materials Using the Calibrated End-Loaded Split (C-ELS) Test and an Effective Crack Length Approach, International Organization for Standardization, 2014.

[19] B.R.K. Blackman, A.J. Kinloch, M. Paraschi, The determination of the mode II adhesive fracture resistance, $G_I IC$, of structural adhesive joints: an effective crack length approach, Eng. Fract. Mech. 72 (6) (2005) 877–897, http://dx.doi.org/10.1016/j.engfracmech.2004.08.007.

[20] Dong Quan, Josu Labarga Urdaniz, Alojz Ivankovic, Enhancing mode-I and mode-II fracture toughness of epoxy and carbon fibre reinforced epoxy composites using multi-walled carbon nanotubes, Mater. Des. 143 (2018) 81–92, http://dx.doi.org/10.1016/j.matdes.2018.01.051.

[21] Dong Quan, Francesca Bologna, Gennaro Scarselli, Alojz Ivankovic, Neal Murphy, Interlaminar fracture toughness of aerospace-grade carbon fibre reinforced plastics interleaved with thermoplastic veils, Compos. A 128 (2020) 105642, http://dx.doi.org/10.1016/j.compositesa.2019.105642.

[22] Victor A. Ramirez, Paul J. Hogg, William W. Sampson, The influence of the nonwoven veil architectures on interlaminar fracture toughness of interleaved composites, Compos. Sci. Technol. 110 (2015) 103–110, http://dx.doi.org/10.1016/j.compscitech.2015.01.016.